Optical properties of sila-adamantane nanoclusters from density-functional theory

Olli Lehtonen

Department of Engineering Physics and Mathematics, Helsinki University of Technology, P.O. Box 2200,
FIN-02015 HUT, Espoo, Finland

Dage Sundholm

Department of Chemistry, University of Helsinki, P.O. Box 55 (A.I. Virtasen Aukio 1), FIN-00014 University of Helsinki, Finland

The molecular structure of $Si_{14}C_{24}H_{72}$, which is a recently synthesized sila-adamantane cluster (Si_{10}) capped by twelve methyl groups and four trimethylsilyl groups, was optimized at the density-functional theory level using the Becke-Perdew functional and triple-ζ quality basis sets augmented with polarization functions. The molecular structures of related hydrogen-terminated silicon nanoclusters with a sila-adamantane cage at the cluster center were optimized at the same level of theory. The electronic excitation spectra of these species were studied at the time-dependent density-functional theory level by employing many different functionals of generalized-gradient approximation type, but also two hybrid functionals were used. The computational study comprises $Si_{10}H_{16}$, $Si_{14}H_{24}$, $Si_{22}H_{40}$, $Si_{26}H_{48}$, $Si_{38}H_{72}$, $Si_{82}H_{72}$, and $Si_{106}H_{120}$ clusters. The clusters consisting of one capped adamantane cage have bright states among the ten lowest dipole allowed transitions, whereas for the two largest silicon nanoclusters with fused adamantane units, the oscillator strengths of the 50 lowest states are about two orders of magnitude weaker than for the small ones. Coupled-cluster calculations of the excitation spectrum of $Si_{10}H_{16}$ support the results obtained at the density-functional theory levels.

I. INTRODUCTION

Sila-adamantane is a tricyclic cage-shaped Si_{10} cluster that can be considered to be the smallest repeat unit of crystallized silicon. The sila-adamantane cage capped with methyl and trimethylsilyl substituents was recently synthesized as an independent molecule.[1] This is an important achievement in silicon chemistry since sila-adamantane molecules bridge the gap between well-defined chemically synthesized silicon compounds and less strictly characterized silicon nanoclusters, which show promise in future optical devices. Thus, the sila-adamantane molecule is anticipated to provide new information about the optical properties of silicon compounds in the transition between silicon molecules and nanoclusters.

Even though silicon nanoclusters (Si-NCs) have been extensively studied both experimentally and computationally, the detailed mechanisms of the light absorption and emission processes of Si-NCs are not yet understood. Allan *et al.* suggested a mechanism involving self-trapped surface states,[2] but this mechanism has not been supported by more recent calculations.[3–5] For porous silicon, a variety of other luminescence mechanisms has been proposed.[6] Some them have also been related to the luminescence of Si-NCs. The experimental absorption thresholds are rather well reproduced in many computational studies.[4,5,7–14] The Franck-Condon (FC) shifts, obtained by optimizing the structure of the excited state using, e.g, the time-dependent density-functional theory (TDDFT) approach, have also in some cases been found to yield luminescence energies in good agreement with measurements,[4,5] whereas in other calculations the obtained FC shifts are significantly larger than one would expect from the photoluminescence experiments; no consensus concerning the Franck-Condon shifts has yet been reached.[4,5,15–17]

The band strengths, i.e., the oscillator strengths obtained in the calculations of electronic absorption and photolumi-

nescence spectra of Si-NCs, are weak as compared to experimental data,[4,5,18] whereas experimentally, the Si-NCs are found to be very bright with stronger photoluminescence (PL) emission intensities than fluorescein.[14,19,20] The PL intensity is related to the oscillator strength of the emitting state. However, in the case of PL, factors other than oscillator strengths have to be considered in the simulation of the luminescence strengths, since the intensity depends on the deexcitation route and the population of the levels. Both radiative and nonradiative transitions might play important roles.[21] The final luminescence spectrum is a result of several competing coupled processes and can only be obtained by solving the rate equations for them. However, a recent experimental study suggests that the luminescence intensity is merely due to large oscillator strengths and the high quantum efficiency. Thus, the nonradiative relaxation rate is vanishingly small compared to the rate along the radiative recombination channel.[14]

In our previous calculations of absorption and emission spectra of Si-NCs, the obtained intensities for the low-lying states were too small as compared to experimental values. One plausible explanation for the discrepancy between the calculated oscillator strengths and detected PL intensity is that different Si-NCs have been investigated experimentally and computationally. In our previous computational studies, the Si-NCs were constructed starting out from a Si tetrahedron at the cluster center. In this work, we are inspired by the recently synthesized sila-adamantane structure.[1] We focus on alternative Si-NC structures consisting of a sila-adamantane cage (Si_{10}) at the cluster center. Calculations on the bare Si_{10} cluster[22] and on the hydrogen-terminated $Si_{10}H_{16}$ cluster[17,23–29] have been reported previously, whereas here we extend the computational studies to include the methyl and trimethylsilyl capped sila-adamantane molecule, five
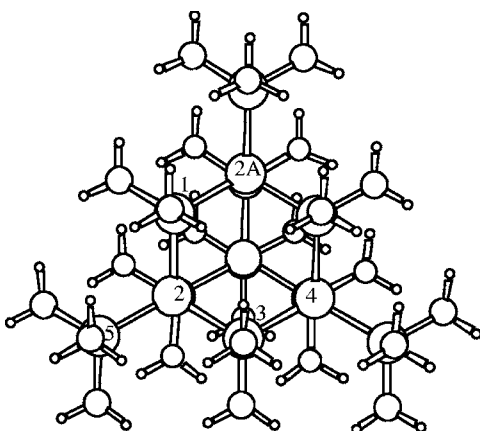
FIG. 1. The molecular structure of sila-adamantane ($Si_{14}C_{24}H_{72}$) optimized at the BP/TZVP level. The atom numbers of the silicons of the Si_{10} cage (1,2,2A,3,4) and of the silyl group (5) used in Table I are indicated.

FIG. 2. The molecular structure of $Si_{10}H_{16}$ optimized at the BP/TZVP level.

hydrogen-terminated and silyl-capped sila-adamantane based nanoclusters, and two hydrogen-terminated and silyl-capped Si-NCs with 13 fused Si_{10} cages.

II. COMPUTATIONAL METHODS

The optimization of the molecular structure of the sila-adamantane cage capped with methyl and methylated silyl groups as well as of the sila-adamantane–based silicon nanoclusters were performed at the density-functional theory (DFT) level using the gradient corrected Becke-Perdew (BP) functional,[30–32] which belongs to the functionals of the generalized-gradient approximation (GGA) type. All electrons were explicitly considered in the DFT calculations. The Karlsruhe triple-ζ valence quality basis sets augmented with polarization functions (TZVP)[33] were used as the default basis set.

The electronic excitation spectra were calculated using time-dependent density-functional theory (TDDFT).[34–37] The resolution of the identity (RI) approximation (also called density fitting) was employed in order to speed up the GGA computations.[38] The errors caused by the RI approximation

TABLE I. Comparison of experimental and calculated bond lengths (in Å) and angles (in degrees) for $Si_{14}C_{24}H_{72}$. The BP functional and TZVP basis sets were used in the optimization of the cluster structure.

Structural parameter[a]	Expt.[b]	Calc.
Si(1)-Si(2)	2.3545(7)	2.397
Si(2)-Si(5)	2.3635(7)	2.411
Si(2)-Si(1)-Si(2A)	110.34(2)	110.7
Si(3)-Si(2)-Si(1)	108.75(2)	108.9
Si(1)-Si(2)-Si(5)	110.07(2)	110.1
Si(2A)-Si(1)-Si(2)-Si(3)	59.89(3)	59.3
Si(5)-Si(2)-Si(3)-Si(4)	179.673(17)	180.0

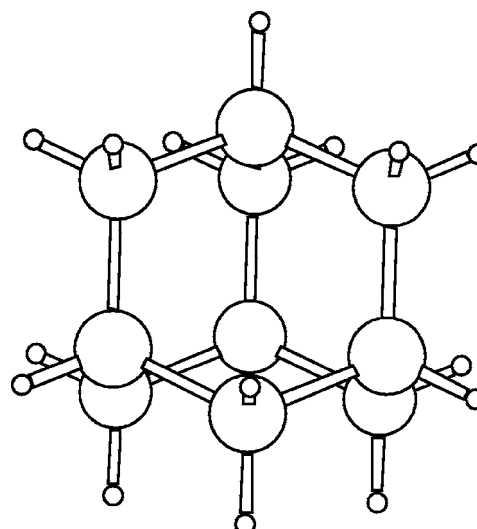[a]The atom numbers are indicated in Fig. 1.
[b]Reference 1.

are only minute and in practice they do not affect the results at all. The electronic excitation energies of the silicon clusters were obtained at the GGA level using the BP functional, the Perdew-Burke-Ernzerhof (PBE) functional,[39] and Becke's gradient corrected exchange functional (BLYP)[32] in combination with the Lee-Yang-Parr correlation functional.[40] The local-density approximation (LDA) using the Slater-Vosko-Wilk-Nusair (SVWN) functional was also used in the TDDFT calculations.[30,41,42] Two hybrid functionals were used in the TDDFT calculations, namely Becke's three-parameter hybrid functional[43] with the Lee-Yang-Parr correlation functional[40] (B3LYP) and the Perdew-Burke-Ernzerhof hybrid functional (PBE0).[44] The oscillator strengths are obtained from transition dipole moments calculated in the length representation as described in Ref. 36.

Dunning's augmented triple-ζ (aug-cc-pVTZ) and quadruple-ζ (aug-cc-pVQZ) basis sets[45,46] were used to check the basis-set convergence. For Si, we used the aug-cc-pV(Q+d)Z basis set with an extra d function.[47] The abbreviation aug-cc-pVQZ denotes here these basis sets. The Karlsruhe triple-ζ valence basis set augmented with a double set of polarization functions (TZVPP) and the Karlsruhe quadruple-ζ valence quality basis sets augmented with $4d2f1g$ polarization functions (QZVP) taken from Dunning's aug-cc-pV(Q+d)Z basis set were also employed.

In addition, the excitation spectrum of the unsubstituted hydrogen-terminated sila-adamantane cluster, $Si_{10}H_{16}$, was studied at the coupled-cluster singles (CCS) and the coupled-cluster approximate singles and doubles (CC2) level.[48,49] In the CCS and CC2 calculations on $Si_{10}H_{16}$, the TZVP and TZVPP quality basis sets were employed. The TURBOMOLE program package[50] has been used in all calculations.

III. RESULTS

A. Structures

In the BP/TZVP optimizations of the molecular structures of the $Si_{14}C_{24}H_{72}$, $Si_{10}H_{16}$, $Si_{14}H_{24}$, $Si_{22}H_{40}$, $Si_{26}H_{48}$, $Si_{38}H_{72}$,
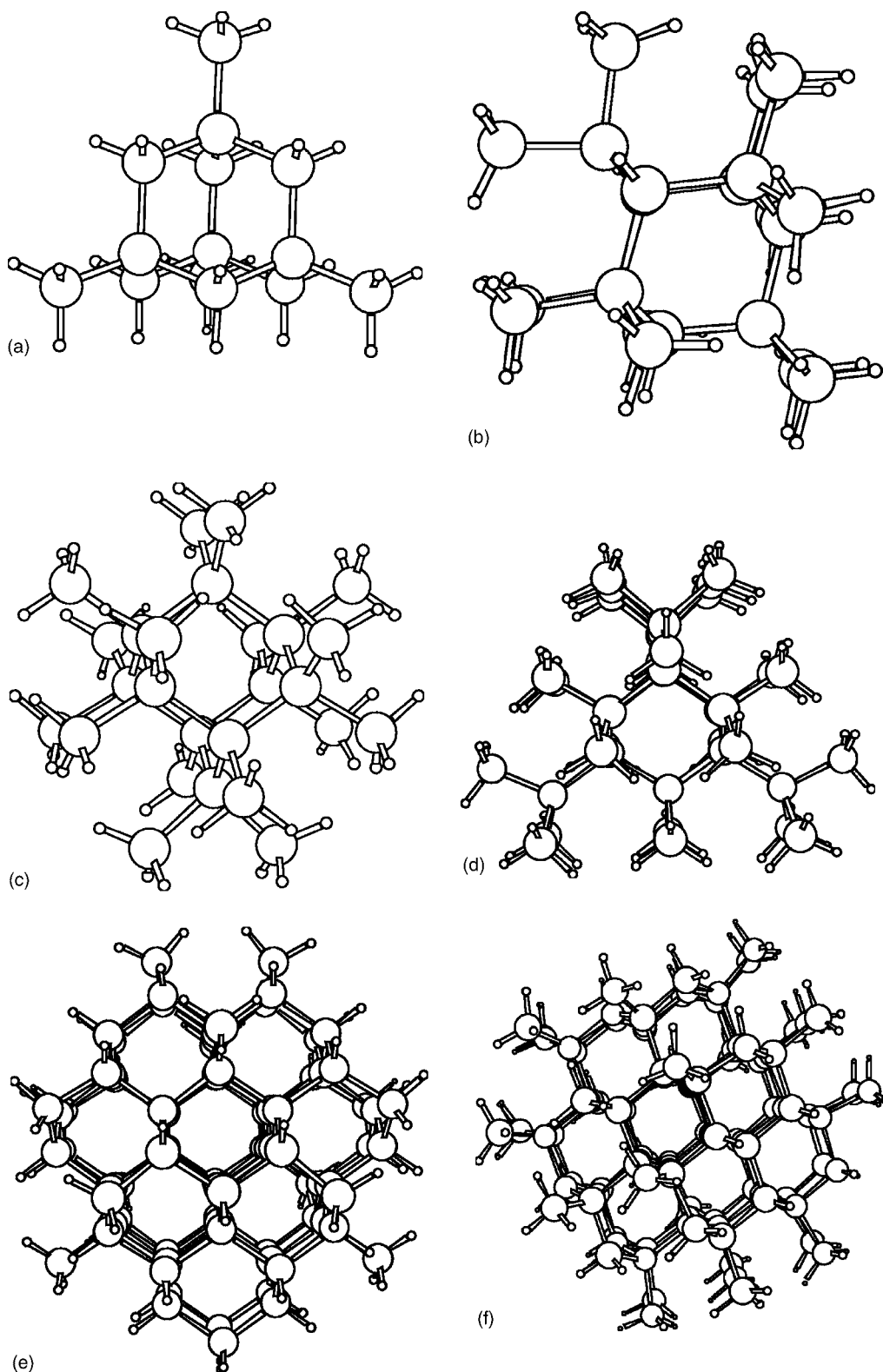
FIG. 3. The molecular structure of (a) $Si_{14}H_{24}$, (b) $Si_{22}H_{40}$, (c) $Si_{26}H_{48}$, (d) $Si_{38}H_{72}$, (e) $Si_{82}H_{72}$, and (f) $Si_{106}H_{120}$ optimized at the BP/TZVP level.

$Si_{82}H_{72}$, and $Si_{106}H_{120}$ clusters, it was assumed that they belong to the T_d point group; merely electronic transition to T_2 states are dipole allowed. The optimized structures for the methyl and trimethylsilyl capped sila-adamantane cage ($Si_{14}C_{24}H_{72}$) are shown in Fig. 1 and the hydrogen-terminated sila-adamantane based Si-NCs are shown in Figs. 2 and 3. The convergence criteria for the geometry optimization are $<10^{-3}$ hartree/bohr for the gradient and

TABLE II. The lowest dipole allowed excitation energies (in eV) of $Si_{10}H_{16}$ calculated at DFT and CC levels using different basis-set sizes.

Basis set	SVWN	BP	PBE	BLYP	B3LYP	PBE0	CCS	CC2
TZVP	5.02	5.12	5.09	5.18	5.73	5.77	7.36	6.35
TZVPP	4.94	5.04	5.01	5.10	5.65	5.68	7.22	6.14
QZVP	4.80	4.91	4.86	4.95	5.50	5.54		
aug-cc-pVTZ	4.83	4.95	4.89	4.97	5.51	5.56		
aug-cc-pVQZ[a]	4.76	4.88	4.82	4.90	5.45	5.49		5.95[b]

[a]For Si, the aug-cc-pV(Q+d)Z basis set with one tight d function was used.[47]
[b]Extrapolated value. The estimated experimental excitation threshold is 5.9 eV.

$<10^{-6}$ hartree for the energy. The optimized structures of $Si_{10}H_{16}$ and $Si_{14}C_{24}H_{72}$ were confirmed to be energy minima by calculating the harmonic vibrational frequencies.

As seen in Table I, the calculated and measured $Si_{14}C_{24}H_{72}$ structures agree well. The calculated bond lengths are 4–5 pm longer than those deduced from the x-ray measurement,[1] and the calculated bond lengths and torsion angles differ by only 0.1–0.5 degrees from the experimental values.

The studied Si-NC structures are derived from $Si_{14}C_{24}H_{72}$ by modifications of the substituents. The smallest Si-NC is $Si_{10}H_{16}$, which consists of a Si_{10} cage surrounded by hydrogens. The $Si_{14}H_{24}$ cluster is obtained from $Si_{14}C_{24}H_{72}$ by replacing all methyl groups by hydrogens and in $Si_{38}H_{72}$ the carbons are replaced by silicons. The $Si_{22}H_{40}$ cluster is obtained by replacing the methylated silyl groups by hydrogens and the remaining eight methyl groups by silyl groups. The $Si_{26}H_{48}$ cluster is obtained by replacing the methyl groups of the methylated silyl groups by silyl groups and the remaining methyl groups are replaced by hydrogens. The two largest clusters, $Si_{82}H_{72}$ and $Si_{106}H_{120}$, consist of fused Si_{10} units. They have 12 sila-adamantane cages around the central Si_{10} cage. In $Si_{82}H_{72}$, the dangling Si bonds are saturated with 12 disilane (Si_2H_4) units, 4 silyl groups, and 12 hydrogens. $Si_{106}H_{120}$ is derived from $Si_{82}H_{72}$ by replacing 24 of the hydrogens with 24 silyl groups.

B. Benchmarking the accuracy

The excitation threshold for the unsubstituted sila-adamantane cage ($Si_{10}H_{16}$) calculated at the CC2/TZVPP level is 6.14 eV. An extensive benchmark study of the excitation energies of silanes showed that the lowest dipole allowed excitation energies obtained at the CC2/TZVPP level are about 0.2 eV larger than the excitation energies obtained in the basis-set limit calculation.[51] The obtained excitation threshold for $Si_{10}H_{16}$ at the CC2/TZVP level is 6.35 eV, which is 0.21 eV larger than the CC2/TZVPP value. The difference between the CC2/TZVP and CC2/TZVPP excitation energies is of the same magnitude as for the silanes and one can therefore expect the CC2/TZVPP excitation energies for $Si_{10}H_{16}$ to be about 0.2 eV larger than the CC2 energies obtained in the basis-set limit calculation. The benchmark study also showed that excitation energies for silanes calculated at the CC2 level also are in close agreement with experimental results.[51] The lowest excitation energy for Si_3H_8 of 6.68 eV calculated at the CC2 level in the basis-set limit calculation was only 0.05 eV larger than the experimental value of 6.63 eV.[52] Thus, by adding the basis-set and correlation corrections to the CC2/TZVPP value, one obtains an estimated experimental excitation threshold for $Si_{10}H_{16}$ of about 5.9 eV.

At the LDA/GGA DFT level and in the DFT calculations using hybrid functionals employing TZVP basis sets, the

TABLE III. The lowest dipole allowed excitation energies (E in eV) of $Si_{14}C_{24}H_{72}$ and the corresponding oscillator strengths (f) calculated at DFT levels using TZVP basis sets. The molecular structure was optimized at the BP/TZVP level.

SVWN		BP		PBE		BLYP		B3LYP		PBE0	
E	f	E	f	E	f	E	f	E	f	E	f
4.27	0.01	4.42	0.02	4.39	0.02	4.48	0.02	5.06	0.05	5.10	0.06
4.29	0.02	4.44	0.02	4.42	0.01	4.51	0.00	5.12	0.11	5.17	0.15
4.47	0.15	4.62	0.16	4.60	0.15	4.66	0.19	5.34	0.27	5.41	0.09
4.58	0.00	4.74	0.00	4.72	0.01	4.83	0.00	5.47	0.08	5.54	0.42
4.69	0.08	4.84	0.09	4.83	0.10	4.88	0.03	5.54	0.66	5.60	0.69
4.80	0.02	4.96	0.17	4.94	0.12	4.97	0.00	5.62	0.01	5.74	0.03
4.86	0.20	5.13	0.02	5.06	0.09	5.06	0.42	5.80	0.14	5.92	0.42
5.12	0.83	5.30	1.04	5.27	0.95	5.33	0.78	5.87	1.04	6.09	0.57
5.24	0.00	5.38	0.00	5.36	0.00	5.42	0.03	6.17	0.01	6.25	0.06
5.30	0.13	5.50	0.03	5.47	0.03	5.45	0.13	6.23	0.00	6.36	0.11

TABLE IV. The lowest dipole allowed excitation energies (E in eV) of $Si_{10}H_{16}$ and the corresponding oscillator strengths (f) calculated at CCS and CC2 levels using TZVP and TZVPP quality basis sets. The molecular structure was optimized at the BP/TZVP level.

CCS TZVP		CC2 TZVP		CCS TZVPP		CC2 TZVPP	
E	f	E	f	E	f	E	f
7.36	0.008	6.35	0.001	7.22	0.004	6.14	0.002
7.65	0.001	6.53	0.001	7.53	0.001	6.58	0.105
7.92	0.002	6.76	0.070	7.83	0.011	6.83	0.210
8.21	2.533	6.99	0.068	8.12	1.964	6.88	0.464
8.25	0.015	7.06	0.919	8.18	0.091	6.99	0.065
8.41	0.952	7.17	0.004	8.29	1.021	7.22	0.371
9.02	0.182	7.36	0.380	8.95	0.208	7.35	0.051
9.20	0.523	7.46	0.077	9.14	0.715	7.61	0.191
9.37	1.781	7.84	0.000	9.23	1.334	7.76	0.373
9.49	1.173	7.96	0.960	9.35	1.164	7.87	0.180

lowest dipole-allowed excitation energies for $Si_{10}H_{16}$ are 5.02–5.18 and 5.73–5.77 eV, respectively, depending on the functional used. Thus, the excitation energies calculated, for example, at the PBE0/TZVP level are due to error cancellation only 0.1 eV smaller than the estimated excitation threshold. The excitation energies obtained using the B3LYP functional are 0.03–0.05 eV smaller than the corresponding PBE0 values. At the GGA DFT levels, the excitation energies are 0.6–0.8 eV smaller than the PBE0 values. By increasing the basis-set size, the excitation thresholds calculated at the DFT levels become too small as compared to the optical gap estimated from the CC2 calculations. The excitation energies obtained at the GGA DFT/aug-cc-pVQZ level are 4.76–4.90 eV, i.e., about 1 eV smaller than the estimated excitation threshold, whereas the B3LYP/aug-cc-pVQZ and PBE0/aug-cc-pVQZ calculations yield optical gaps of 5.45 and 5.49 eV, respectively, which are about 0.4 eV smaller than the extrapolated experimental value of 5.9 eV. The results of the benchmark calculations on $Si_{10}H_{16}$ are summarized in Table II.

For Si_3H_8, the excitation energy calculated at the PBE0/TZVP level is 6.65 eV, which is in excellent agreement with the experimental value of 6.63 eV. The excitation threshold for Si_3H_8 calculated at the GGA DFT/TZVP levels is 6.24–6.31 eV, i.e., 0.3–0.4 eV too small as compared to the experimental data. The excitation thresholds for Si_3H_8 calculated at t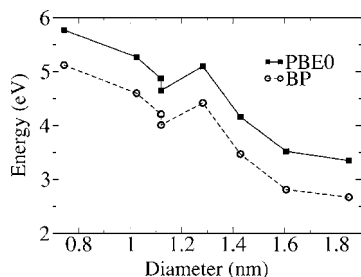he GGA DFT/aug-cc-pVQZ levels are in the range of 5.93–6.08 eV, and in the B3LYP/aug-cc-pVQZ and PBE0/aug-cc-pVQZ calculations the corresponding values are 6.25 and 6.36 eV, respectively. Thus, at the basis-set limit, the PBE0 and B3LYP excitation energies for Si_3H_8 are, as for $Si_{10}H_{16}$, underestimated by 0.3–0.4 eV.

C. The absorption spectrum of $Si_{14}C_{24}H_{72}$

The electronic excitation spectrum for sila-adamantane capped with methyl and trimethylsilyl groups has a strong absorption maximum at 222 nm or 5.59 eV.[1] In the DFT/

FIG. 4. The optical gap (in eV) calculated at the PBE0/TZVP and BP/TZVP levels as a function of the cluster diameter in nm.
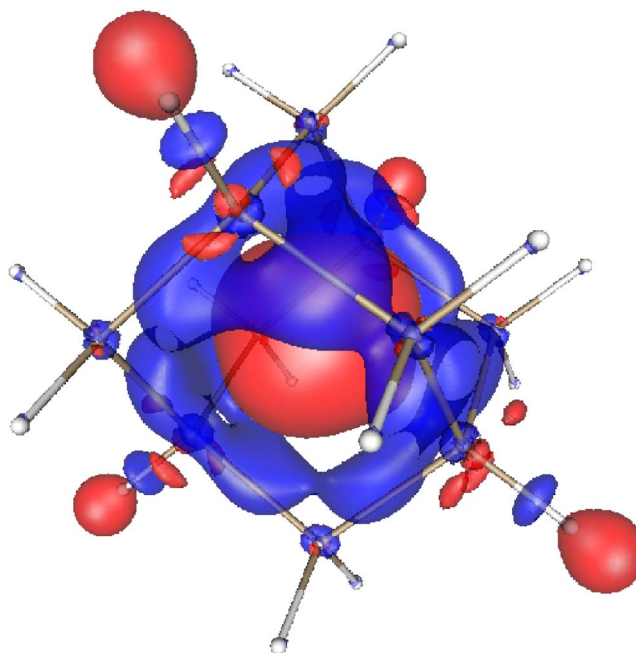

FIG. 5. (Color online) The change in the charge density upon excitation for $Si_{10}H_{16}$ calculated at the B3LYP/TZVP level. The electron accumulation is indicated with dark gray (red) and the charge depletion regions with light gray (blue). An isodensity value of 0.001 $e\text{Å}^{-1}$ was used. The figure was produced with the GOPENMOL program (Refs. 54 and 55).

TABLE V. The lowest dipole allowed excitation energies (E in eV) of $Si_{10}H_{16}$ and the corresponding oscillator strengths (f) calculated at DFT levels using TZVP basis sets. The molecular structure was optimized at the BP/TZVP level.

SVWN		BP		PBE		BLYP		B3LYP		PBE0	
E	f	E	f	E	f	E	f	E	f	E	f
5.02	0.00	5.12	0.00	5.09	0.00	5.18	0.00	5.73	0.00	5.77	0.00
5.20	0.03	5.34	0.01	5.32	0.02	5.36	0.00	5.90	0.00	6.00	0.01
5.29	0.03	5.39	0.05	5.37	0.05	5.43	0.05	6.07	0.07	6.16	0.09
5.43	0.00	5.64	0.00	5.59	0.00	5.66	0.01	6.28	0.05	6.37	0.04
5.57	0.00	5.73	0.00	5.69	0.00	5.71	0.00	6.39	0.06	6.50	0.00
5.58	0.01	5.76	0.02	5.72	0.02	5.79	0.01	6.42	0.00	6.53	0.17
5.76	0.01	5.93	0.00	5.90	0.00	5.90	0.00	6.54	0.03	6.71	0.05
5.93	0.15	6.05	0.18	6.03	0.16	6.01	0.21	6.59	0.35	6.78	0.26
6.18	0.05	6.34	0.01	6.31	0.01	6.34	0.08	7.04	0.00	7.15	0.01
6.23	0.01	6.39	0.12	6.36	0.11	6.41	0.05	7.09	0.35	7.25	0.35

TZVP calculations using the GGA functionals, the excitation threshold is obtained at 4.27–4.48 eV, whereas at the B3LYP/TZVP and PBE0/TZVP levels the obtained excitation thresholds are 5.06 and 5.10 eV, respectively. The observed strong absorption maximum probably corresponds to the fourth and fifth excited states, whose oscillator strengths at the PBE0/TZVP level are 0.42 and 0.69, respectively. The corresponding excitation energies calculated at the PBE0/TZVP level are 5.54 and 5.60 eV. At the GGA DFT level, three strong transitions appear at 4.47–4.66, 4.86–5.06, and 5.12–5.33 eV, whereas in the B3LYP/TZVP calculation, the two lowest strong bands appear at 5.34 and 5.54 eV. The excitation energies calculated at the PBE0/TZVP and B3LYP/TZVP levels agree well with experimental results. However, the use of larger basis sets would again yield too small excitation energies. The excitation energies calculated at the GGA DFT level using the TZVP basis sets are more than 0.5 eV too small as compared to experiment, showing the limitations of the applicability of the GGA functionals on Si-NCs. The excitation energies of the ten lowest dipole-allowed states of $Si_{14}C_{24}H_{72}$ calculated at different DFT levels are given in Table III.

For $Si_{14}C_{24}H_{72}$, the lowest excited state was found to belong to the T_1 irreducible representation. However, the excitation energy for the first T_1 state calculated at the BP/TZVP level is only 0.01 eV below the lowest T_2 state. For the Si-NCs covered with hydrogens only, the lowest excited states are T_2 states.

D. Sila-adamantane based Si-NCs

The lowest dipole-allowed excitation energies of the hydrogen-terminated Si-NCs with a sila-adamantane cage at the center have been calculated at the DFT level using a LDA functional, three GGA functionals, and two hybrid functionals. The TZVP basis sets were employed in the DFT calculations, since according to the benchmark calculations the B3LYP and PBE0 functional in combination with TZVP yield excitation energies in good agreement with available experimental data. For $Si_{10}H_{16}$, the excitation energies were

TABLE VI. The lowest dipole allowed excitation energies (E in eV) of $Si_{14}H_{24}$ and the corresponding oscillator strengths (f) calculated at DFT levels using TZVP basis sets. The molecular structure was optimized at the BP/TZVP level.

SVWN		BP		PBE		BLYP		B3LYP		PBE0	
E	f	E	f	E	f	E	f	E	f	E	f
4.46	0.09	4.60	0.10	4.57	0.10	4.64	0.11	5.22	0.19	5.27	0.20
4.60	0.00	4.74	0.00	4.71	0.00	4.78	0.00	5.37	0.04	5.43	0.06
4.66	0.04	4.81	0.03	4.78	0.03	4.85	0.03	5.41	0.06	5.48	0.06
4.97	0.09	5.08	0.11	5.06	0.11	5.08	0.13	5.76	0.21	5.88	0.21
5.09	0.00	5.23	0.01	5.20	0.01	5.25	0.01	5.88	0.01	6.00	0.00
5.26	0.18	5.37	0.15	5.35	0.16	5.37	0.11	6.01	0.52	6.12	0.74
5.36	0.00	5.55	0.00	5.52	0.00	5.60	0.12	6.18	0.06	6.30	0.03
5.50	0.07	5.61	0.15	5.59	0.13	5.62	0.02	6.25	0.14	6.34	0.08
5.63	0.10	5.76	0.11	5.73	0.10	5.78	0.19	6.42	0.46	6.55	0.31
5.71	0.07	5.84	0.08	5.81	0.09	5.86	0.04	6.59	0.00	6.69	0.00

TABLE VII. The lowest dipole allowed excitation energies (E in eV) of $Si_{22}H_{40}$ and the corresponding oscillator strengths (f) calculated at DFT levels using TZVP basis sets. The molecular structure was optimized at the BP/TZVP level.

SVWN		BP		PBE		BLYP		B3LYP		PBE0	
E	f	E	f	E	f	E	f	E	f	E	f
4.08	0.02	4.21	0.02	4.18	0.02	4.31	0.02	4.87	0.05	4.87	0.06
4.25	0.09	4.37	0.09	4.35	0.10	4.43	0.07	5.07	0.39	5.12	0.44
4.29	0.03	4.41	0.06	4.38	0.05	4.47	0.07	5.07	0.00	5.14	0.03
4.40	0.01	4.60	0.01	4.58	0.01	4.65	0.01	5.25	0.02	5.33	0.03
4.43	0.00	4.61	0.00	4.59	0.00	4.66	0.00	5.30	0.00	5.39	0.00
4.46	0.01	4.63	0.01	4.61	0.01	4.68	0.01	5.32	0.00	5.41	0.01
4.55	0.01	4.69	0.01	4.67	0.01	4.73	0.01	5.37	0.01	5.46	0.00
4.63	0.01	4.75	0.01	4.73	0.01	4.79	0.11	5.45	0.02	5.55	0.04
4.67	0.24	4.79	0.26	4.78	0.25	4.82	0.19	5.46	0.50	5.59	0.49
4.97	0.07	5.09	0.04	5.07	0.04	5.11	0.08	5.79	0.22	5.92	0.17

also calculated at the CCS and CC2 levels using TZVP and TZVPP basis sets. The obtained energies and oscillator strengths are given in Table IV. The excitation energies and oscillator strengths for the Si-NCs calculated at the DFT levels are summarized in Tables V–IX. The excitation threshold decreases with the size of the Si-NC. At the PBE0/TZVP level, the first dipole-allowed excitations are 5.77, 5.27, 4.87, 4.65, and 4.16 eV for the $Si_{10}H_{16}$, $Si_{14}H_{24}$, $Si_{22}H_{40}$, $Si_{26}H_{48}$, and $Si_{38}H_{72}$ clusters, respectively. The oscillator strengths vary less systematically. The oscillator strengths of the first transition of $Si_{14}H_{24}$ and $Si_{38}H_{72}$ are significantly larger than for the other Si-NCs.

The optical gap as a function of the cluster diameter is shown in Fig. 4. The energy threshold decreases smoothly with the cluster size except for the methyl and trimethylsilyl capped sila-adamantane, whose optical gap is about 0.8 eV larger than one would obtain for a Si-NC of the same size. The methyl substituents are inactive capping groups that do not participate in the excitation process, whereas the silyl groups extend electron delocalization and lower the excitation threshold.

In previous computational studies of the absorption and emission spectra of Si-NCs, we found that the oscillator strengths for the lowest excited states of the Si-NCs are small,[4,8] especially when one considers the fact that the Si-NCs are strongly luminescent.[19,20] For the optimized structure of the lowest excited state, the calculated oscillator strength is also small.[4,5] Based on the calculated data, one would not expect Si-NCs to be strongly luminescent. The Si-NCs considered here differ from the previous ones in the sense that they have a sila-adamantane cage at the cluster center. The present calculations show that the absorption spectra calculated for Si-NCs consisting of one capped Si_{10} cage involve strong low-lying transitions.

The oscillator strengths for $Si_{10}H_{16}$ calculated at coupled-cluster and DFT levels using the TZVP and TZVPP basis sets show considerable variations depending on the computational level. The first dipole-allowed transition has at all computational levels a very small oscillator strength. At the CC2/TZVPP level, the second to fourth excited states have oscillator strengths larger than 0.1. At the DFT level or at the CC2 level employing TZVP quality basis sets, the first three

TABLE VIII. The lowest dipole allowed excitation energies (E in eV) of $Si_{26}H_{48}$ and the corresponding oscillator strengths (f) calculated at DFT levels using TZVP basis sets. The molecular structure was optimized at the BP/TZVP level.

| SVWN		BP		PBE		BLYP		B3LYP		PBE0	
E	f	E	f	E	f	E	f	E	f	E	f
3.86	0.00	4.01	0.00	3.98	0.00	4.10	0.01	4.64	0.01	4.65	0.00
3.95	0.02	4.07	0.03	4.05	0.03	4.15	0.03	4.72	0.05	4.75	0.05
3.96	0.01	4.09	0.01	4.08	0.00	4.17	0.00	4.73	0.02	4.76	0.03
4.17	0.00	4.33	0.00	4.31	0.00	4.39	0.00	5.01	0.00	5.06	0.00
4.21	0.00	4.34	0.00	4.33	0.00	4.41	0.01	5.05	0.06	5.13	0.08
4.23	0.00	4.37	0.00	4.35	0.00	4.43	0.00	5.07	0.01	5.14	0.00
4.32	0.05	4.45	0.06	4.44	0.06	4.49	0.06	5.12	0.08	5.23	0.06
4.50	0.00	4.62	0.01	4.60	0.00	4.68	0.00	5.32	0.05	5.39	0.07
4.63	0.10	4.75	0.11	4.74	0.10	4.77	0.12	5.42	0.20	5.54	0.13
4.71	0.01	4.86	0.00	4.83	0.00	4.91	0.01	5.56	0.09	5.65	0.23
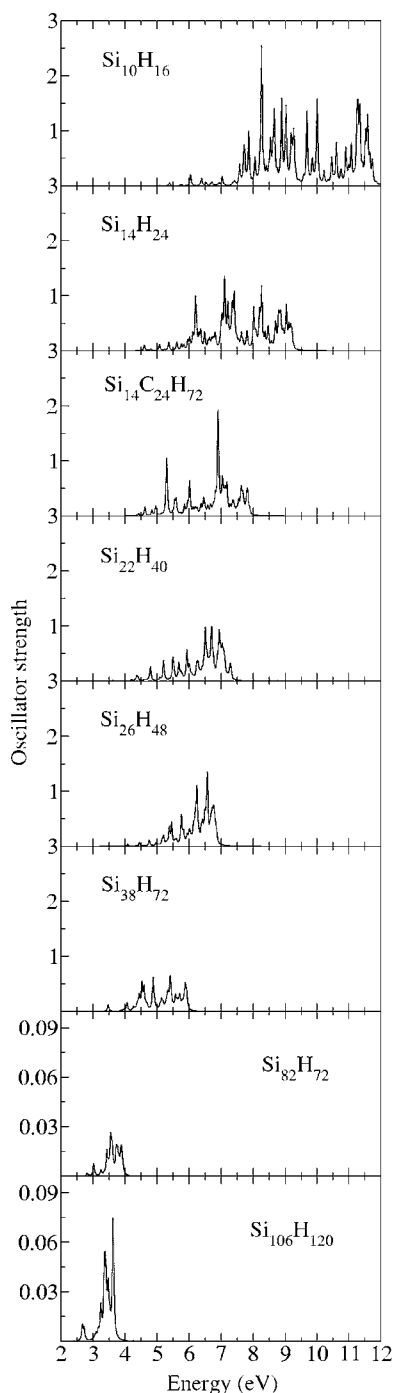
FIG. 6. The electronic absorption spectra for the sila-adamantane–based clusters obtained using excitation energies and oscillator strengths calculated at the BP/TZVP level. Note the different scale in the two lowest plots.

transitions are very weak. The use of larger basis sets in the DFT calculations does not significantly affect the size of the oscillator strengths. The excitation energies and oscillator strengths obtained for $Si_{10}H_{16}$ at the coupled-cluster and DFT levels are given in Tables IV and V.

In the sila-adamantane based Si-NCs, the first transition involves a charge transfer from the peripheral parts of the cluster into the adamantane cage. The charge-density difference between the ground- and excited-state densities for $Si_{10}H_{16}$ is shown in Fig. 5. The areas with electron accumulation are indicated with dark gray (red) and the charge depletion regions with light gray (blue). Similar plots (not shown) for the other transitions do not reveal why some transitions are more intense than others. The first excited state for $Si_{14}H_{24}$ involving the charge transfer to the Si_{10} cage has an oscillator strength of 0.2. The fourth, sixth, and ninth states are also bright. For $Si_{22}H_{40}$, the first transition involving the charge transfer to the Si_{10} cage is weak, whereas the second excited state is the first bright state. The ninth and tenth states have also large oscillator strengths. For $Si_{26}H_{48}$, all low-lying states are weak. The ninth and tenth states are the first bright ones in the $Si_{26}H_{48}$ spectrum. The largest sila-adamantane cluster considered, i.e., $Si_{38}H_{72}$ has five strong transitions among the six lowest states. The second excited state has a small oscillator strength. The calculated excitation energies and oscillator strengths for $Si_{14}H_{24}$, $Si_{22}H_{40}$, $Si_{26}H_{48}$, and $Si_{38}H_{72}$ are summarized in Tables VI–VIII and X, respectively.

E. Si-NCs with fused Si_{10} units

The $Si_{82}H_{72}$ and $Si_{106}H_{120}$ clusters consist of 12 fused Si_{10} units around the central Si_{10} cage. The excitation energies and oscillator strengths for $Si_{82}H_{72}$ and $Si_{106}H_{120}$ were calculated at the DFT levels using the different functionals and TZVP basis sets. The excitation thresholds calculated at the PBE0/TZVP level are 3.52 and 3.35 eV. For the Si-NCs with fused sila-adamantane units, no strong low-lying transitions were obtained. The calculated excitation energies and oscillator strengths of the ten lowest states of $Si_{82}H_{72}$ and $Si_{106}H_{120}$ are given in Tables X and XI. In Fig. 6, the calculated electronic absorption spectra are compared to those obtained for the Si-NCs consisting of one sila-adamantane unit. The absorption spectra are derived from the excitation energies and oscillator strengths calculated at the BP/TZVP level. The 100 lowest excitation energies of T_2 symmetry were considered for the smaller clusters, whereas for $Si_{82}H_{72}$ and $Si_{106}H_{120}$, the transitions to the 50 lowest T_2 states were taken into account. The spectra are broadened by a Lorentzian line-shape function of width 50 meV. The band strengths of the fused sila-adamantane clusters are two orders of magnitude smaller than for the sila-adamantane clusters with only one Si_{10} cage. The lowest states of the fused sila-adamantane clusters have as small oscillator strengths as the $Si_{29}H_{24}$, $Si_{29}H_{36}$, and $Si_{35}H_{36}$ clusters studied previously.[4,5,8] Thus, the experimentally observed strong luminescence from Si-NCs is unlikely due to sila-adamantane based Si-NCs. Reboredo *et al.* also found in their study that the surface chemistry of Si-NCs is practically independent on the cluster structure in the core of the cluster.[53]

IV. CONCLUSIONS

The present computational study shows that excitation energies for Si-NCs are underestimated at the DFT level also when hybrid functionals are employed. In the basis-set limit, the B3LYP and PBE0 functionals yield excitation energies that are about 0.4 eV smaller than experimental results. By using the PBE0 functional in combination with TZVP basis

TABLE IX. The lowest dipole allowed excitation energies (E in eV) of $Si_{38}H_{72}$ and the corresponding oscillator strengths (f) calculated at DFT levels using TZVP basis sets. The molecular structure was optimized at the BP/TZVP level.

SVWN		BP		PBE		BLYP		B3LYP		PBE0	
E	f	E	f	E	f	E	f	E	f	E	f
3.36	0.11	3.47	0.12	3.45	0.12	3.54	0.14	4.12	0.27	4.16	0.26
3.71	0.00	3.85	0.00	3.84	0.00	3.93	0.00	4.50	0.01	4.53	0.01
3.78	0.00	3.90	0.01	3.89	0.01	3.97	0.03	4.56	0.16	4.61	0.17
3.84	0.04	3.97	0.03	3.96	0.03	4.04	0.01	4.69	0.08	4.75	0.11
3.90	0.00	4.02	0.00	4.00	0.00	4.07	0.01	4.76	0.18	4.83	0.15
3.94	0.13	4.06	0.15	4.05	0.14	4.12	0.18	4.81	0.09	4.91	0.10
4.07	0.00	4.23	0.00	4.21	0.00	4.31	0.07	4.94	0.10	4.99	0.01
4.14	0.07	4.27	0.07	4.25	0.07	4.34	0.01	4.97	0.27	5.06	0.33
4.17	0.03	4.31	0.01	4.30	0.01	4.38	0.00	5.05	0.16	5.14	0.31
4.22	0.04	4.35	0.01	4.33	0.01	4.40	0.01	5.09	0.01	5.16	0.01

sets, the obtained excitation energies are in close agreement with experiment due to cancellation of errors. Excitation energies obtained at the GGA DFT levels are rather independent of the functional used, but in the basis-set limit the GGA excitation energies are about 1 eV too small as compared to experiment. Coupled-cluster approximate singles and doubles (CC2) calculations yield in the basis-set limit very accurate excitation energies for Si-NCs. However, CC2 calculations in combination with large basis sets are so far computationally too expensive to be applicable on nanosized Si-NCs.

The molecular structure for the sila-adamantane molecule capped with methyl and trimethylsilyl groups optimized at the BP/TZVP level agrees well with experiment. The obtained bond lengths obtained are 4–5 pm longer than those deduced from the x-ray structure.[1] The excitation energies for sila-adamantane calculated at the PBE0/TZVP level are also in good agreement with experimental data. The observed strong absorption maximum at 222 nm (5.59 eV) (Ref. [1]) can be assigned the fourth and fifth excited states

with large oscillator strengths of 0.42 and 0.69, respectively. The corresponding excitation energies, calculated at the PBE0/TZVP level, are 5.54 and 5.60 eV. The excitation threshold for dipole-allowed transitions of $Si_{14}C_{24}H_{72}$ calculated at the PBE0/TZVP level is 5.10 eV.

A comparison of the optical gaps for $Si_{14}C_{24}H_{72}$ of 5.10 eV, $Si_{38}H_{72}$ of 4.16 eV, and for $Si_{14}H_{24}$ of 5.27 eV shows that the methyl groups affect the optical gap only slightly (0.17 eV), whereas the silyl groups contribute to the electron delocalization of the Si-NC and thereby lower the excitation threshold by almost 1 eV.

For the hydrogen-terminated Si-NCs with only one Si_{10} unit, strong low-lying dipole-allowed transitions appear among the ten lowest states, whereas for the fused sila-adamantane clusters, the oscillator strengths are almost two orders of magnitude weaker. Thus, the oscillator strengths of the fused sila-adamantane clusters are of the same magnitude as for the previously studied Si-NCs built from a tetrahedrally coordinated silicon atom in the cluster center.

TABLE X. The lowest dipole allowed excitation energies (E in eV) of $Si_{82}H_{72}$ and the corresponding oscillator strengths (f) calculated at DFT levels using TZVP basis sets. The molecular structure was optimized at the BP/TZVP level.

SVWN		BP		PBE		BLYP		B3LYP		PBE0	
E	f	E	f	E	f	E	f	E	f	E	f
2.66	0.001	2.81	0.002	2.78	0.001	2.93	0.002	3.53	0.003	3.52	0.003
2.70	0.000	2.85	0.000	2.81	0.000	2.97	0.000	3.56	0.000	3.54	0.000
2.72	0.000	2.87	0.000	2.83	0.000	2.99	0.000	3.57	0.000	3.55	0.000
2.88	0.006	3.02	0.007	2.98	0.007	3.12	0.008	3.76	0.018	3.77	0.019
2.91	0.001	3.04	0.001	3.01	0.001	3.14	0.002	3.78	0.000	3.80	0.000
3.01	0.000	3.16	0.000	3.12	0.000	3.28	0.000	3.93	0.000	3.91	0.000
3.10	0.000	3.23	0.000	3.19	0.000	3.32	0.000	4.01	0.002	4.04	0.002
3.13	0.003	3.25	0.003	3.22	0.003	3.35	0.003	4.04	0.006	4.07	0.005
3.18	0.001	3.33	0.001	3.30	0.001	3.44	0.001	4.09	0.004	4.11	0.006
3.23	0.000	3.37	0.000	3.34	0.000	3.48	0.000	4.15	0.001	4.15	0.003

TABLE XI. The lowest dipole allowed excitation energies (E in eV) of $Si_{106}H_{120}$ and the corresponding oscillator strengths (f) calculated at DFT levels using TZVP basis sets. The molecular structure was optimized at the BP/TZVP level.

SVWN		BP		PBE		BLYP		B3LYP		PBE0	
E	f	E	f	E	f	E	f	E	f	E	f
2.54	0.008	2.67	0.009	2.63	0.009	2.78	0.011	3.37	0.025	3.35	0.025
2.58	0.000	2.71	0.001	2.68	0.001	2.81	0.001	3.43	0.010	3.41	0.007
2.59	0.006	2.72	0.007	2.69	0.006	2.84	0.008	3.46	0.003	3.44	0.002
2.60	0.000	2.74	0.000	2.70	0.000	2.87	0.000	3.47	0.001	3.48	0.002
2.64	0.001	2.78	0.001	2.74	0.001	2.89	0.001	3.55	0.001	3.55	0.002
2.83	0.000	2.96	0.000	2.93	0.000	3.08	0.001	3.73	0.000	3.73	0.000
2.86	0.001	2.98	0.001	2.95	0.001	3.08	0.000	3.78	0.000	3.81	0.000
2.91	0.001	3.05	0.001	3.01	0.001	3.14	0.000	3.80	0.004	3.84	0.004
2.94	0.001	3.06	0.001	3.04	0.001	3.16	0.001	3.84	0.000	3.87	0.001
2.98	0.003	3.10	0.003	3.08	0.003	3.16	0.006	3.88	0.004	3.94	0.002

[1] J. Fischer, J. Baumgartner, and C. Marschner, Science **310**, 825 (2005).

[2] G. Allan, C. Delerue, and M. Lannoo, Phys. Rev. Lett. **76**, 2961 (1996).

[3] A. Puzder, A. J. Williamson, F. A. Reboredo, and G. Galli, Phys. Rev. Lett. **91**, 157405 (2003).

[4] D. Sundholm, Phys. Chem. Chem. Phys. **6**, 2044 (2004).

[5] O. Lehtonen and D. Sundholm, Phys. Rev. B **72**, 085424 (2005).

[6] L. T. Canham, in *Properties of Porous Silicon*, edited by L. T. Canham (INSPEC, The Institution of Electrical Engineers, London, 1997), pp. 247–255.

[7] C. S. Garoufalis, A. D. Zdetsis, and S. Grimme, Phys. Rev. Lett. **87**, 276402 (2001).

[8] D. Sundholm, Nano Lett. **3**, 847 (2003).

[9] A. Puzder, A. J. Williamson, J. C. Grossman, and G. Galli, J. Chem. Phys. **117**, 6721 (2002).

[10] C. S. Garoufalis and A. D. Zdetsis, Phys. Chem. Chem. Phys. **8**, 808 (2006).

[11] L. Mitas, J. Terrien, R. Twesten, G. Belomoin, and M. H. Nayfeh, Appl. Phys. Lett. **78**, 1918 (2001).

[12] E. W. Draeger, J. C. Grossman, A. J. Williamson, and G. Galli, Phys. Rev. Lett. **90**, 167402 (2003).

[13] S. Rao, J. Sutin, R. Clegg, E. Gratton, M. H. Nayfeh, S. Habbal, A. Tsolakidis, and R. M. Martin, Phys. Rev. B **69**, 205319 (2004).

[14] A. Smith, Z. H. Yamani, N. Roberts, J. Turner, S. R. Habbal, S. Granick, and M. H. Nayfeh, Phys. Rev. B **72**, 205307 (2005).

[15] A. Franceschetti and S. T. Pantelides, Phys. Rev. B **68**, 033313 (2003).

[16] A. Puzder, A. J. Williamson, J. C. Grossman, and G. Galli, J. Am. Chem. Soc. **125**, 2786 (2003).

[17] E. Degoli, G. Cantele, E. Luppi, R. Magri, D. Ninno, O. Bisi, and S. Ossicini, Phys. Rev. B **69**, 155411 (2004).

[18] X. Yang, X. L. Wu, S. H. Li, H. Li, T. Qiu, Y. M. Yang, P. K. Chu, and G. G. Siu, Appl. Phys. Lett. **86**, 201906 (2005).

[19] O. Akcakir, J. Terrien, G. Belomoin, N. Barry, J. D. Muller, E. Gratton, and M. H. Nayfeh, Appl. Phys. Lett. **76**, 1857 (2000).

[20] M. H. Nayfeh, in *Conference Proceedings Vol. 71: Atoms, Molecules and Quantum Dots in Laser Fields: Fundamental Processes*, edited by N. Bloembergen, N. Rahman, and A. Rizzo (Societa' Italiana di Fisica, Bologna, 2001), pp. 83–96.

[21] D. Kovalev, H. Heckler, G. Polisski, and F. Koch, Phys. Status Solidi B **215**, 871 (1999).

[22] T. T. Rantala, D. A. Jelski, and T. F. George, Chem. Phys. Lett. **232**, 215 (1995).

[23] R. Broer, G. Aissing, and W. C. Nieuwpoort, Int. J. Quantum Chem., Quantum Chem. Symp. **22**, 297 (1988).

[24] M. Hirao and T. Uda, Surf. Sci. **306**, 87 (1994).

[25] I. Vasiliev, S. Ogut, and J. R. Chelikowsky, Phys. Rev. B **65**, 115416 (2002).

[26] L. X. Benedict, A. Puzder, A. J. Williamson, J. C. Grossman, G. Galli, J. E. Klepeis, J. Y. Raty, and O. Pankratov, Phys. Rev. B **68**, 085310 (2003).

[27] E. Luppi *et al.*, Opt. Mater. (Amsterdam, Neth.) **27**, 1008 (2004).

[28] Y. B. Ge and J. D. Head, Mol. Phys. **103**, 1035 (2005).

[29] F. Pichierri, Chem. Phys. Lett. **421**, 319 (2006).

[30] S. H. Vosko, L. Wilk, and M. Nusair, Can. J. Phys. **58**, 1200 (1980).

[31] J. P. Perdew, Phys. Rev. B **33**, 8822 (1986).

[32] A. D. Becke, Phys. Rev. A **38**, 3098 (1988).

[33] A. Schäfer, C. Huber, and R. Ahlrichs, J. Chem. Phys. **100**, 5829 (1994).

[34] R. Bauernschmitt and R. Ahlrichs, Chem. Phys. Lett. **256**, 454 (1996).

[35] R. Bauernschmitt, M. Häser, O. Treutler, and R. Ahlrichs, Chem. Phys. Lett. **264**, 573 (1997).

[36] F. Furche, J. Chem. Phys. **114**, 5982 (2001).

[37] F. Furche and R. Ahlrichs, J. Chem. Phys. **117**, 7433 (2002).

[38] K. Eichkorn, O. Treutler, H. Öhm, M. Häser, and R. Ahlrichs, Chem. Phys. Lett. **240**, 283 (1995).

[39] J. P. Perdew, K. Burke, and M. Ernzerhof, Phys. Rev. Lett. **77**, 3865 (1996).

[40] C. Lee, W. Yang, and R. G. Parr, Phys. Rev. B **37**, 785 (1988).

[41] P. A. M. Dirac, Proc. Cambridge Philos. Soc. **26**, 376 (1930).

[42] J. C. Slater, Phys. Rev. **81**, 385 (1951).

[43] A. D. Becke, J. Chem. Phys. **98**, 5648 (1993).

[44] J. P. Perdew, K. Burke, and M. Ernzerhof, J. Chem. Phys. **105**, 9982 (1996).

[45] T. H. Dunning, Jr., J. Chem. Phys. **90**, 1007 (1989).

[46] D. E. Woon and T. H. Dunning, Jr., J. Chem. Phys. **98**, 1358 (1993).

[47] T. H. Dunning, Jr., K. A. Peterson, and A. K. Wilson, J. Chem. Phys. **114**, 9244 (2001).

[48] O. Christiansen, H. Koch, and P. Jørgensen, Chem. Phys. Lett. **243**, 4041 (1995).

[49] C. Hättig and F. Weigend, J. Chem. Phys. **113**, 5154 (2000).

[50] R. Ahlrichs, M. Bär, M. Häser, H. Horn, and C. Kölmel, Chem. Phys. Lett. **162**, 165 (1989), current version: see http://www.turbomole.de

[51] O. Lehtonen and D. Sundholm (unpublished results).

[52] U. Itoh, Y. Yasutake, H. Onuki, N. Washida, and T. Ibuki, J. Chem. Phys. **85**, 4867 (1986).

[53] F. A. Reboredo and G. Galli, J. Phys. Chem. B **109**, 1072 (2005).

[54] L. Laaksonen, J. Mol. Graphics **10**, 33 (1992).

[55] D. L. Bergman, L. Laaksonen, and A. Laaksonen, J. Mol. Graphics Modell. **15**, 301 (1997).